Nicotine stabilization in composite sodium alginate based wafers and films for nicotine replacement therapy.

Obinna C. Okeke, Joshua S. Boateng*

Department of Pharmaceutical Chemical and Environmental Sciences, Faculty of Engineering and Science, University of Greenwich at Medway, Central Avenue, Chatham Maritime, ME4 4TB, Kent, UK.

* Correspondence: Dr Joshua Boateng (J.S.Boateng@gre.ac.uk; joshboat40@gmail.com)

Abstract:

Composite wafers and films comprising HPMC and sodium alginate (SA) were formulated for nicotine (NIC) replacement therapy via the buccal route. Magnesium aluminium silicate (MAS) was added in different concentration ratios (0.25, 0.5, 0.75) to stabilize NIC and its effect on mechanical properties, internal and surface morphology, physical form, thermal properties, swelling, mucoadhesion, drug content and release behaviour of the formulations was investigated. MAS changed the physico-mechanical properties of the composite formulations causing a decrease in mechanical hardness, collapsed wafer pores, increased roughness of film surface, increase in crystallinity and decreased mucoadhesion of the wafers. However, MAS increased swelling in both films and wafers as well as interaction between NIC and SA, which increased drug-loading capacity. Further, MAS resulted in rapid and slow release of NIC from wafer and films respectively. The results suggest that the ideal formulation for the stabilization of NIC in the composite formulations was MAS 0.25.

Keywords: Buccal delivery; Magnesium Aluminium Silicate (MAS); Nicotine; Nicotine replacement therapy; Sodium alginate.

1 Introduction

Nicotine has been utilised as an active ingredient in the development of NIC replacement therapy (NRT) via the oral mucosa (chewing gum, sublingual tablets, lozenges), nasal mucosa (nasal spray and inhalers) and the skin (transdermal patch). NIC liquid is volatile, alkaline and colourless with two well-separated pK_a values of 3.04 and 7.84, which can form diprotonated, mono-protonated and neutral NIC species in an acid, neutral or basic solvent respectively (Pongjanyakul & Suksri, 2009). These species can permeate membranes such as nasal, buccal and sublingual mucosae with

unionized species showing higher permeation than ionized forms (Nair, Chetty, Ho, & Chien, 1997).

The oral mucosa of delivery has gained increased interest because of its ability to avoid gastric acid, enzymes in the small intestine and first pass metabolism in the liver, common with the conventional oral route (Sattar, Sayed, & Lane, 2014). The buccal mucosa is highly vascular, less vulnerable to irritation and has a lower amount of enzyme activities compared to intestinal, rectal, vaginal and nasal mucosae (Boateng & Okeke, 2014). Though the use of the buccal mucosa for NIC delivery has been demonstrated in NIC chewing gum, Nicorette®, a large percentage of the drug is swallowed before achieving complete absorption (Nair et al., 1997; Adrian, Olin, Dalhoff & Jacobsen, 2006; Benowitz, Jacob, & Savanapridi, 1987).

Alternative buccal delivery systems, which can be utilised in NRT using mucoadhesive polymers have been under investigation including films (Aguzzi, Cerezo, Viseras, & Caramella, 2007) and wafers (Aguzzi et al., 2007; Boateng & Areago, 2014) and demonstrated improved functional properties when different polymers were combined. Hydroxypropylmethylcellulose (HPMC) and sodium alginate (SA) have been widely used as mucoadhesive polymers in the development of buccal-adhesive drug delivery systems (Boateng & Areago, 2014; Manivannan, Balasubramaniam, Anand, Sandeep, & Rajkumar, 2008; Adhikari, Nayak, Nayak, & Mohanty, 2010; Pandey, Hingawe, Das, & Patil, 2014; Khan, Boateng, Mitchell, & Trivedi, 2015). HPMC is a hydrophilic non-ionic semi-synthetic polymer widely used in the pharmaceutical and food industries while SA is a poly-anionic polysaccharide polymer made up of alginic acid (a polyuronic acid composed of mannuronic and guluronic acid residues), extracted from brown seaweed. HPMC-SA composites were reported for the

formulation of buccal NIC tablets for smoking cessation (İkinci, Şenel, Wilson, & Şumnu, 2004).

The challenges posed by NIC are its volatility and oxidative degradation of the free base. To address these challenges, there has been research into the adsorption of NIC onto several materials such as cellulose powder (Mihranyan, Andersson, & Ek, 2004), cation exchange resins (Rakić et al., 2010) and inorganic clays such as magnesium aluminium silicate (MAS) (Pongjanyakul & Suksri, 2009). In particular, polymer-clay composites having improved mechanical properties, thermal behaviour and modified drug release have attracted interest in the field of drug delivery (Aguzzi et al., 2007; Gilman, 1999; Pavlidou & Papaspyrides, 2008).

MAS results from the combination of natural smectites (montmorillonite and saponite clays) that forms a layered structure (Rowe, Sheskey, & Owen, 2006; Pongjanyakul & Suksri, 2009), comprising three-lattice layers of octahedral alumina or magnesia and two tetrahedral silica. Upon hydration, the MAS layered structure separates, exposing the weakly positively charged edges and negatively charged faces. This can readily interact with amine drugs such as NIC, as well as demonstrate electrostatic interaction, which contributes to slow drug release in formulations (Pongjanyakul & Suksri, 2009; Rowe et al., 2006). MAS incorporated into NIC loaded single polymer (SA) based films demonstrated interaction of MAS with anionic SA polymer as well as increase in NIC retention within the films (Pongjanyakul & Suksri, 2010).

In this study, composite SA based films and wafers containing different concentrations of MAS, loaded with NIC were characterised and compared for the first time. The hypothesis is that the presence of SA and MAS within a composite

formulation will stabilize NIC and result in high drug loading suitable for NRT via the buccal mucosa.

2 Materials and methods

2.1 Materials

Hydroxypropylmethylcellulose - HPMC (Methocel K100 premium LV) and Magnesium aluminium silicate (MAS) were gifts from Colorcon Limited (Dartford, UK) and R.T. Vanderbilt Company Inc (Norwalk, CT, USA) respectively. Sodium hydroxide, potassium dihydrogen phosphate, gelatine were purchased from Fluka Analytical (Buchs, Switzerland). Nicotine (liquid form), sodium alginate –SA (molecular weight 120,000 – 190,000 g/mol, mannuronate/guluronate ratio 1.56), and mucin from porcine stomach were all obtained from Sigma Aldrich (Dorset, UK); sodium acetate, trimethylamine and glycerol were purchased from Fisher Scientific (Loughborough, UK).

2.2 Preparation of composite films

NIC loaded MAS films were prepared in different ratios with a total polymer (HPMC-SA) concentration of 2% w/v. The concentrations of polymers, MAS, plasticizer and drug used in each polymer solution have been summarised in Table 1a. The polymeric solutions for film formulation were prepared by dissolving glycerol (GLY) in 80ml of distilled water while stirring at of 25°C before gradually adding HPMC and SA powder one after the other and stirred between 500-700rpm for 2 hours. MAS on the other hand was dissolved in 20ml of hot distilled water (50°C) for 30 mins, and mixed with the dispersed polymeric solution. The resulting final solutions were left overnight (16-20 hrs) to eliminate air bubbles, NIC added to the MAS composite mixture and stirred at

low rpm (100-200rpm) for 30 mins. 30 g of the NIC loaded MAS solutions were poured into a Petri dish (90mm diameter) and dried in an oven at 30°C for 18-20 hrs.

Table 1: (a) Composition of selected polymer, plasticizer, MAS and NIC used in composite gel for film formulation and (b) Composition of selected polymers, MAS and NIC used in composite gels for formulating wafers.

(a) Films

Sample name	**HPMC (% w/v)**	**SA (% w/v)**	**GLY (% w/v)**	**MAS (% w/v)**	**NIC (g)**
MAS 0.00	1.25	0.75	2.00	0.00	0.20
MAS 0.25	1.25	0.75	2.00	0.25	0.20
MAS 0.50	1.25	0.75	2.00	0.50	0.20
MAS 0.75	1.25	0.75	2.00	0.75	0.20

(b) Wafers

Sample name	**HPMC (% w/v)**	**SA (% w/v)**	**MAS (% w/v)**	**NIC (g)**
MAS 0.00	1.25	0.75	0.00	0.20
MAS 0.25	1.25	0.75	0.25	0.20
MAS 0.50	1.25	0.75	0.50	0.20
MAS 0.75	1.25	0.75	0.75	0.20

2.3 Preparation of composite wafers

NIC loaded HPMC-SA-MAS solutions were prepared in a similar manner to films but without using GLY. The solutions (1g) were poured into each well of a 24 well plate

(diameter 15.5mm). The concentrations of polymers, MAS and drug present in each solution are summarised in Table 1b. The freeze-dried wafers were prepared using an automated lyophilisation cycle, Virtis Advantage XL 70 freeze-dryer (Biopharma process systems, Winchester, UK). The well plates containing the gels were loaded onto the shelves of the freeze-dryer and programmed for freezing, primary drying and secondary drying steps. The freezing step involved cooling the sample from room temperature to 5°C (40 mins), 5°C to -10°C (40 mins), and then from -10°C to -55°C (120 mins). An annealing step was incorporated into the freezing cycle by increasing the temperature from -55°C to -35°C (2 hrs) and then cooling back down to -55°C (3 hrs). Additional freezing was performed at -55°C (1 hr) with a condenser temperature of -55°C under pressure (200mTorr). The primary drying occurred under high pressure of 50mTorr. The temperature was raised from -55°C to -20°C (8 hrs) and further increased from -20°C to -15°C ° (10 hrs). Secondary drying occurred at 50mTorr, from -15°C to 25°C (12.5 hrs).

2.4 Polymer solution properties

The polymeric solutions were analysed for surface stickiness, stringiness and gel strength using a texture analyser (HD plus, Stable Micro System, Surrey, UK) equipped with a 5 kg load cell. A 25mm probe was lowered onto the solution at a speed of 1mm/sec, held for 2 sec, and then withdrawn at a speed of 8mm/sec. The maximum force at withdrawal of probe from sample was recorded as surface stickiness while the distance from the onset and offset of force while moving the probe away from the sample was recorded as stringiness. The viscous ‘gel’ strength was recorded as the maximum force as the probe penetrated the polymeric solution to the required depth.

2.5 Mechanical characterization using texture analysis (TA)

2.5.1 Tensile properties of films

The tensile properties of the films were analysed using a texture analyser (HD plus, Stable Micro System, Surrey, UK) equipped with a 5 kg load cell. The films (dumb-bell shaped) were fixed between two tensile grips of the TA instrument and then stretched at a test speed of 2mm/sec till breaking point. The elongation at break (%), tensile strength and elastic modulus were determined (n=3) (Morales & McConville, 2011).

2.5.2 Mechanical properties of wafers (hardness)

The resistance to compressive deformation (hardness) of the freeze dried wafers was determined using a texture analyser (HD plus, Stable Micro System, Surrey, UK) equipped with a 5 kg load cell. The wafers were compressed to a depth of 2mm using a 2mm cylinder stainless steel probe in compression mode at a speed of 1mm/sec. Wafers were compressed on 5 different sides (n=3).

2.6 Scanning electron microscopy (SEM)

The surface morphology of films and wafers were analysed using a Hitachi SU8030 (Hitachi High-Technologies, Krefeld, Germany) scanning electron microscope. Formulations were cut and placed on an Agar Scientific G301 aluminium pin-type stubs, using an Agar Scientific G3347N double-sided adhesive carbon tape. The films were carbon coated, while wafers were gold coated using a Sputter Coater (Edwards 188 Sputter Coater S1508). The films and wafers were analysed at 2.0kV and 5.0kV accelerating voltage respectively.

2.7 Wafer porosity

Pore analysis was performed in order to evaluate the porosity of wafer structure. The wafers were initially weighed and then immersed in 5ml of ethanol in a glass vial and left to stand for 10 mins to allow complete saturation with ethanol. The vials with ethanol and wafers were degassed to remove air bubbles entrapped in the wafers for 10 mins. The wafers were carefully removed from the solvent, gently wiped to remove excess solvent, and immediately weighed, to minimise loss of ethanol.

The percentage porosity of wafers was calculated using equation 1 below:

$$P = \frac{V_p}{V_g} \times 100 = \frac{W_f - W_i}{\rho_e V_g} \qquad (1)$$

Where

V_p = pore volume

V_g = wafers geometrical volume

W_f = final wafer weight

W_i = initial wafer weight

ρ_e = ethanol density (0.789 g/cm^3)

2.8 X-ray diffraction (*XRD*)

The physical (crystalline/amorphous) form of NIC loaded MAS films and wafers was investigated using a D8 Advantage X-ray diffractometer. Films were cut into small pieces whilst wafers were compressed, placed on the holder and mounted onto the sample cell. For pure starting materials, mylar was used to hold the powders before placing on the sample cell. The samples were analysed in transmission mode at a diffraction angle ranging from 5° to 50° 2θ, step size 0.04°, and scan speed of 0.4s/step.

2.9 Attenuated total reflectance Fourier transform infrared spectroscopy (ATR-FTIR)

ATR-FTIR spectra were obtained from a Perkin Elmer Spectrum instrument equipped with a diamond universal ATR-unit. Strips of films and wafers and polymer powders were separately placed on the ATR diamond crystal and force applied using a pressure clamp to allow adequate contact between the sample and diamond crystal. NIC required no force application as the liquid could form intimate contact with the diamond crystal. The resolutions of the samples were recorded at 4 cm^{-1} within the range of 450-4000 cm^{-1}. Background spectra were subtracted in other to obtain a reliable absorbance of each sample.

2.10 Swelling

The swelling capacities of films and wafers were determined by immersing each formulation into 5ml of phosphate buffered saline (pH 6.8; ionic strength, 0.07M) and change in weight recorded at time intervals of 2 mins up to 30 mins. For every time interval, the medium was carefully removed to obtain an accurate weight of the sample and replaced with fresh medium. Three replicates were performed for each sample and swelling index (%) was calculated using equation 2 (Nair et al., 2013).

$$Swelling\ index = \frac{Ws - Wd}{Wd} \times 100 \qquad (2)$$

Where W_d = dry weight of film or wafer.

W_s = weight of film or wafer after swelling.

2.11 Mucoadhesion

Adhesion test was performed on films and wafers using a TA. HD *plus* texture analyser (Stable micro systems, Surry, UK) in tensile mode and fitted with a 5kg load cell. Films

were cut to match the mathematical area of wafers (a circle with diameter = 15.5mm). The formulations were attached to an adhesive probe (75mm diameter) of the TA instrument using a double-sided adhesive tape. Gelatine solution (6.67% (w/v)) prepared at 70°C (stirred at 500-700rpm) was poured into a Petri dish (86mm diameter) and immediately placed in a fridge overnight (16-20 hrs) to set into solid gel, and 0.5 ml of mucin solution (2% (w/v)) prepared in phosphate buffered saline (pH 6.8; ionic strength, 0.07M) at room temperature was evenly spread on the gelatine gel to represent the buccal mucosa. The probe with formulation attached was lowered to make contact with the model buccal mucosa surface for 60 sec, at an applied force of 1.00N, and then detached. Mucoadhesive strength was determined by the peak adhesive force (PAF) required to detach the sample from the gelatine surface, total work of adhesion (TWA) was determined by the area under the force-distance curve, while cohesiveness represents the distance the samples travelled till they detached from the model buccal surface. Texture Exponent 32® software was used in collecting and processing the data from the TA analyser.

2.12 High performance liquid chromatography (HPLC)

NIC was analysed by HPLC using an Agilent 1200 HPLC instrument (Agilent Technologies, Cheshire, UK) with an auto sampler. The column used was a C-18 reverse-phase column, 4.6 x 250mm (Phenomenex, Cheshire, UK). Trimethylamine, methanol and sodium acetate (88:12:0.5 v/v) were used as mobile phase and pH adjusted to 4.2 using glacial acetic acid. Mobile phase flow rate was 1ml/min and wavelength detection was set at 259nm (Pongjanyakul & Suksri, 2010). The retention time of NIC was detected at approximately 4.5 min. Calibration curve was plotted using standards with NIC concentration ranging from 40µg/ml to 400µg/ml ($R^2=0.9994$).

2.13 Drug content

The content of NIC in NIC loaded MAS films and wafers was assayed by accurately weighing and dissolving films and wafers in 10ml of distilled water. The films and wafers were accurately weighed (20-40mg) and recorded in determining the drug content. The resulting solution was collected into a syringe, filtered through a 0.45µm cellulose acetate membrane, transferred into HPLC vials and placed in HPLC sample chamber and analysed as described above (*n=3*).

2.14 In vitro drug dissolution

In vitro drug dissolution of NIC loaded films and wafers was performed using a Franz-diffusion cell apparatus. The receptor compartment was filled with 8ml of phosphate buffer (pH 6.8) with a mesh (1mm mesh size) on the receptor surface. The donor and receptor compartments were sealed with paraffin to limit evaporation and held together by a pinch clamp. The system was placed on a water bath at 37°C with magnetic stirring at approximately 200rpm. Formulations were accurately cut, weighed (20-40 mg) and placed on the mesh between the donor and receptor compartments. At predetermined time intervals, 0.5ml aliquots of the dissolution media were withdrawn using a 1ml syringe, filtered through a 0.45µm cellulose acetate membrane, transferred into HPLC vials and analysed using HPLC. The aliquot withdrawn was always replaced with fresh buffer solution at 37°C. The percentage cumulative drug released from both films and wafers were calculated and plotted against time (n=3).

Experimental release data was fitted to various kinetic models using representative plots. These plot profiles include: cumulative % drug release vs time (zero order kinetic model); log cumulative of % drug remaining vs time (first order kinetic model); cumulative % drug release vs square root of time (Higuchi model); cube root of drug % remaining in matrix vs time (Hixson-Crowell cube root law); and log

cumulative % drug release vs log time (Korsmeyer-Peppas model). (Dash, Murthy, Nath, & Chowdhury, 2010; Singhvi & Singh, 2011).

2.15 Statistical analysis

The results were expressed as mean (± standard deviation) and statistical analysis was performed using student t-test and / or one-way ANOVA to compare results. The significant differences of data were determined at a level of $p < 0.05$.

3 Results

3.1 Polymer solution properties

The pH of the HPMC-SA solutions was neutral but increased to between pH 9-10 upon addition of NIC. NIC loaded HPMC-SA-MAS solutions were less viscous and therefore flowed easily when poured into both the well plates and Petri-dishes for wafers and films respectively.

Table 2: Surface stickiness, stringiness and gel strength of HPMC-SA-MAS gel formulations

Formulations	*Surface stickiness (g)*	*Stringiness (mm)*	*Gel strength (g)*
MAS 0.00	15.51 ± 9.30	0.80 ± 0.27	804.42 ± 268.81
MAS 0.25	18.98 ± 1.64	0.88 ± 0.08	981.45 ± 111.59
MAS 0.50	4.15 ± 0.39	0.53 ± 0.07	184.09 ± 10.30
MAS 0.75	20.91 ± 0.708	0.85 ± 0.05	541.51 ± 153.24

The HPMC-SA-MAS solutions (Table 2) also demonstrated increase in surface stickiness, stringiness and ‘gel’ strength with initial increase in MAS concentration

from MAS 0.00 to MAS 0.25, but a decrease in stickiness, stringiness and gel strength for MAS 0.50 formulation and a subsequent increase in stickiness, stringiness and 'gel' strength for the MAS 0.75 formulation. Overall, the MAS 0.25 formulation demonstrated the highest value of stringiness and 'gel' strength compared to other formulations, while MAS 0.75 formulation demonstrated the highest value of surface stickiness. However, MAS 0.50 formulation demonstrated the lowest value of stickiness, stringiness and 'gel' strength compared to the other MAS loaded formulations. NIC loaded solutions were transparent with light brown colour but transparency decreased as MAS concentration increased.

3.2 Texture analysis (TA)

3.2.1 Tensile properties of films

Figure 1a shows the tensile profiles of NIC loaded SA based composite films at different MAS concentrations. The tensile strength of NIC loaded SA based composite films ranged from 4.98 ± 0.55N/mm to 6.58 ± 0.15N/mm. There was a gradual increase in tensile strength as the concentration of MAS increased. Films with the lowest concentration of MAS (0.25) showed the lowest tensile strength (4.98 ± 0.55 N/mm) while those with the maximum MAS concentration (0.75) showed the highest tensile strength (6.58 ± 0.15N/mm). There was also a significant difference ($p<0.05$) between MAS 0.25 and MAS 0.75 tensile strength. A gradual increase in elastic modulus was also observed as MAS concentration increased with the highest concentration of MAS (MAS 0.75) exhibiting the highest value (28.04 ± 1.2327N/mm^2) of elastic modulus. A decrease in elongation at break (%) was observed as MAS concentration increased which was most pronounced at the highest concentration of MAS (MAS 0.75) with a value of 16 ± 0.58 %. Composite films with no MAS demonstrated the highest

299 elongation at break (%) of 53 ± 4.27 followed by MAS 0.50 (30 ± 1.85). In general, the
300 concentration of MAS had an effect on the mechanical properties of NIC loaded
301 composite films.
302
303

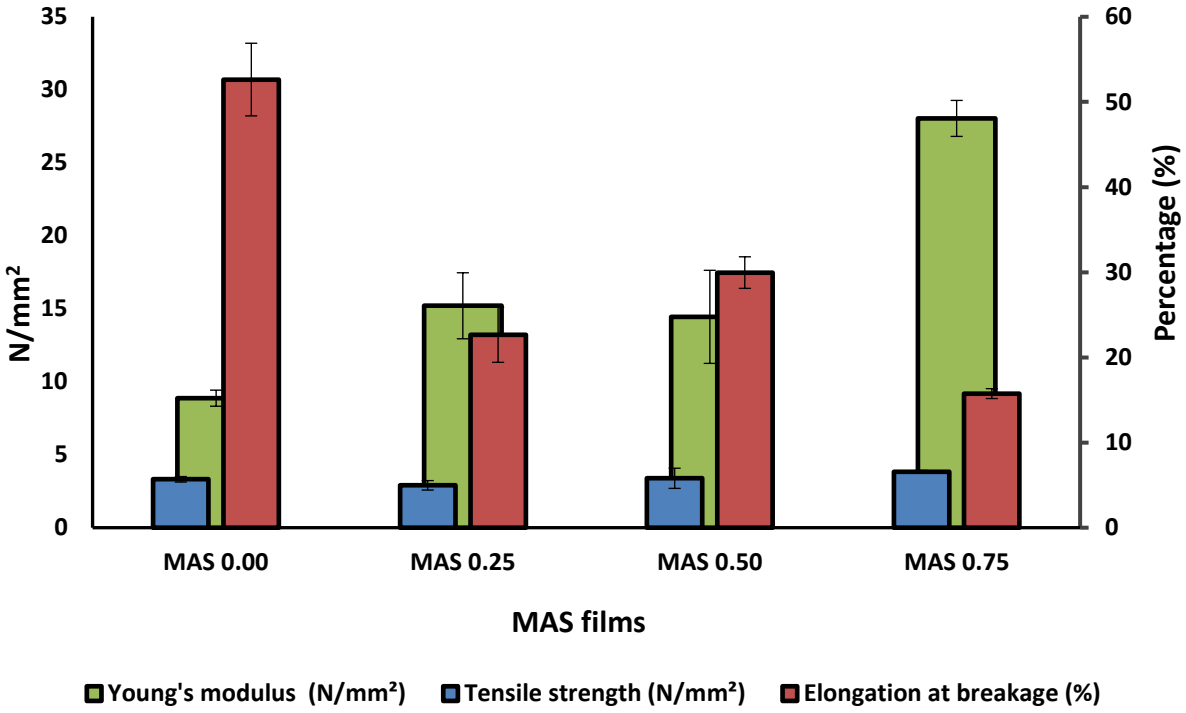

304
305 **(a)**

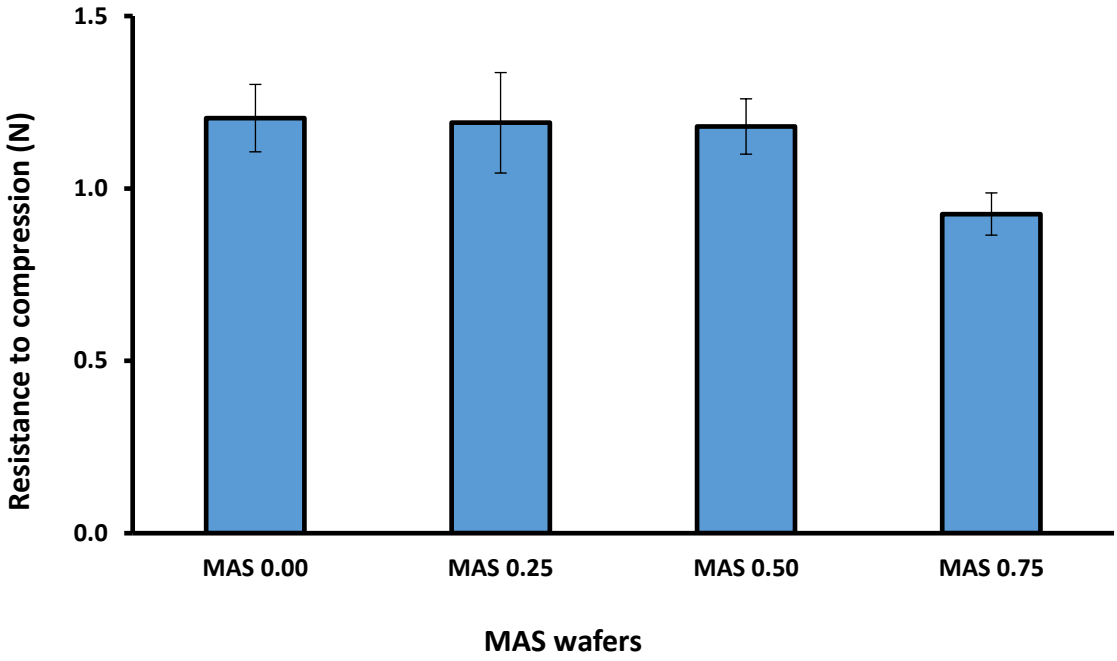

(b)

Figure 1 (a) Tensile properties of NIC loaded films (*n* = 3) and (b) Hardness profiles showing the resistance of NIC loaded wafers (*n* = 3) to compressive deformation forces.

3.2.2 Mechanical properties of wafer (hardness)

Figure 1b shows the hardness profiles of NIC loaded SA based composite wafers at different MAS concentrations. The results showed similar hardness values of 1.20 ± 0.10, 1.19 ± 0.15 and 1.18 ± 0.08N for MAS 0.00, 0.25 and 0.50 wafers respectively, but decreased (0.93 ± 0.06N) for wafers containing the highest amounts of MAS (0.75). The results show that increase in the concentration of MAS up to MAS 0.50 did not affect the resistance of wafer to compression deformation force until the concentration exceeded MAS 0.50 (i.e. MAS 0.75) as demonstrated in Figure 1b.

3.3 Scanning electron microscopy (SEM)

The internal structures and surface morphology of wafers and films, are shown in Figures 2 and 3 respectively. Wafers demonstrated a sponge-like and porous internal structure while the films showed a continuous polymer sheet. The wafers showed

collapsed pore walls as MAS concentration increased with a highly collapsed wall observed at MAS 0.75. The films also demonstrated a rough surface morphology as MAS concentration increased with MAS 0.75 film showing the most uneven surface compared to other films.

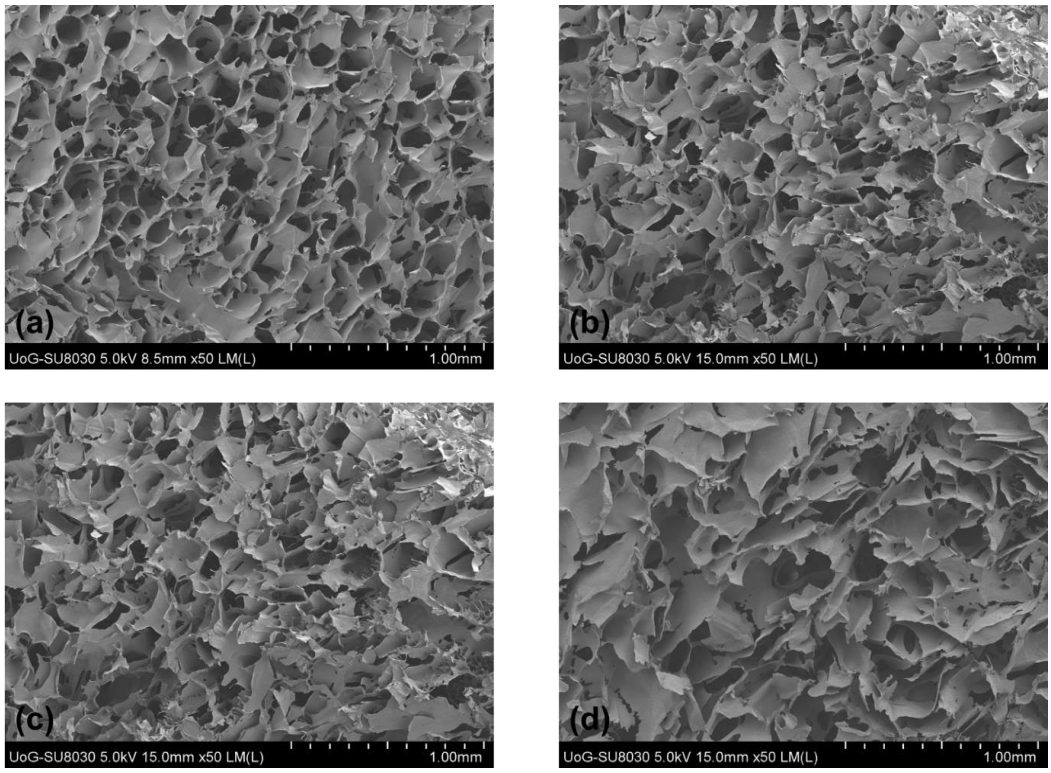

Figure 2 SEM images of NIC loaded wafers containing different amounts of MAS: (a) MAS 0.00 (b) MAS 0.25 (c) MAS 0.50 and (d) MAS 0.75.

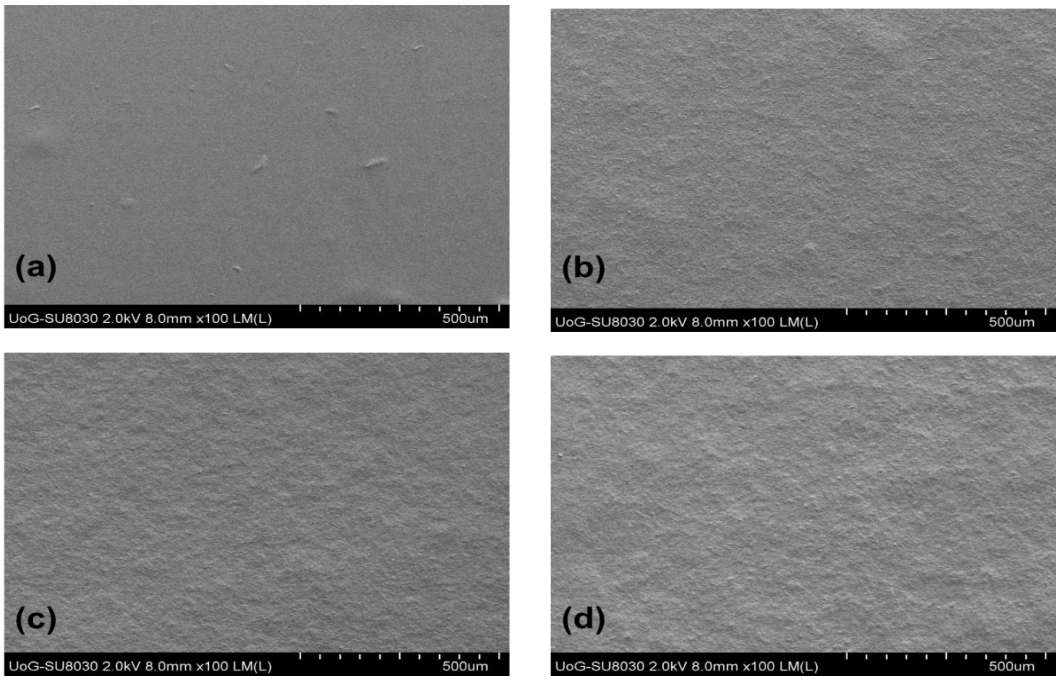

Figure 3 SEM images of NIC loaded films containing different amounts of MAS: (a) MAS 0.00 (b) MAS 0.25 (c) MAS 0.50 and (d) MAS 0.75.

3.4 Wafers porosity

Figure S1 (supplementary data) shows the porosity (%) of SA based composite wafers at different MAS concentrations. The results demonstrated a decrease in porosity as MAS concentration in the formulation increased from MAS 0.00 to 0.50, but showed a sudden increase at maximum MAS concentration (MAS 0.75). However, this cannot be conclusive because of the degree of error observed between MAS 0.50 and 0.75. Generally, the result supports SEM results wafers with a better pore structure and homogeneity observed for HPMC-SA wafer with no MAS present (i.e. MAS 0.00).

3.5 XRD analysis

Figure S2(a) shows XRD transmission diffractograms of pure SA, HPMC, MAS and mylar (Okeke and Boateng, 2016). HPMC and SA demonstrated a broad peak at 2θ between 15° - 24° and 20° - 23° respectively suggesting amorphous structure. Unlike

346 HPMC and SA powders, MAS demonstrated a crystalline form with diffraction peaks at
347 2θ values of 20°, 22°, 23° and 29°, and a broad amorphous peak from 2θ of 34° – 38°.
348 Figure S2(b) showed one crystalline peak at 2θ 23° in NIC loaded composite wafer
349 without MAS (MAS 0.00) but showed three crystalline peaks at 20°, 22°, 23° for all
350 other MAS formulations (i.e. MAS 0.25, 0.50 and 0.75), attributed to the presence of
351 MAS. NIC loaded wafer also demonstrated a broad peak from 2θ 15-24° and from 2θ
352 34° – 38°. NIC loaded film without MAS showed a broad peak from 2θ 15-24° while
353 MAS loaded films (i.e. MAS 0.25, 0.50 and 0.75) showed broad peaks from 15-24°
354 with two crystalline shoulders at 2θ of 20° and 22°.
355

356 ***3.6 ATR-FTIR spectroscopy***

357 ATR-FTIR spectra of SA, HMPC), GLY, NIC, MAS, NIC loaded composite wafers and
358 films are shown in Figure 4.

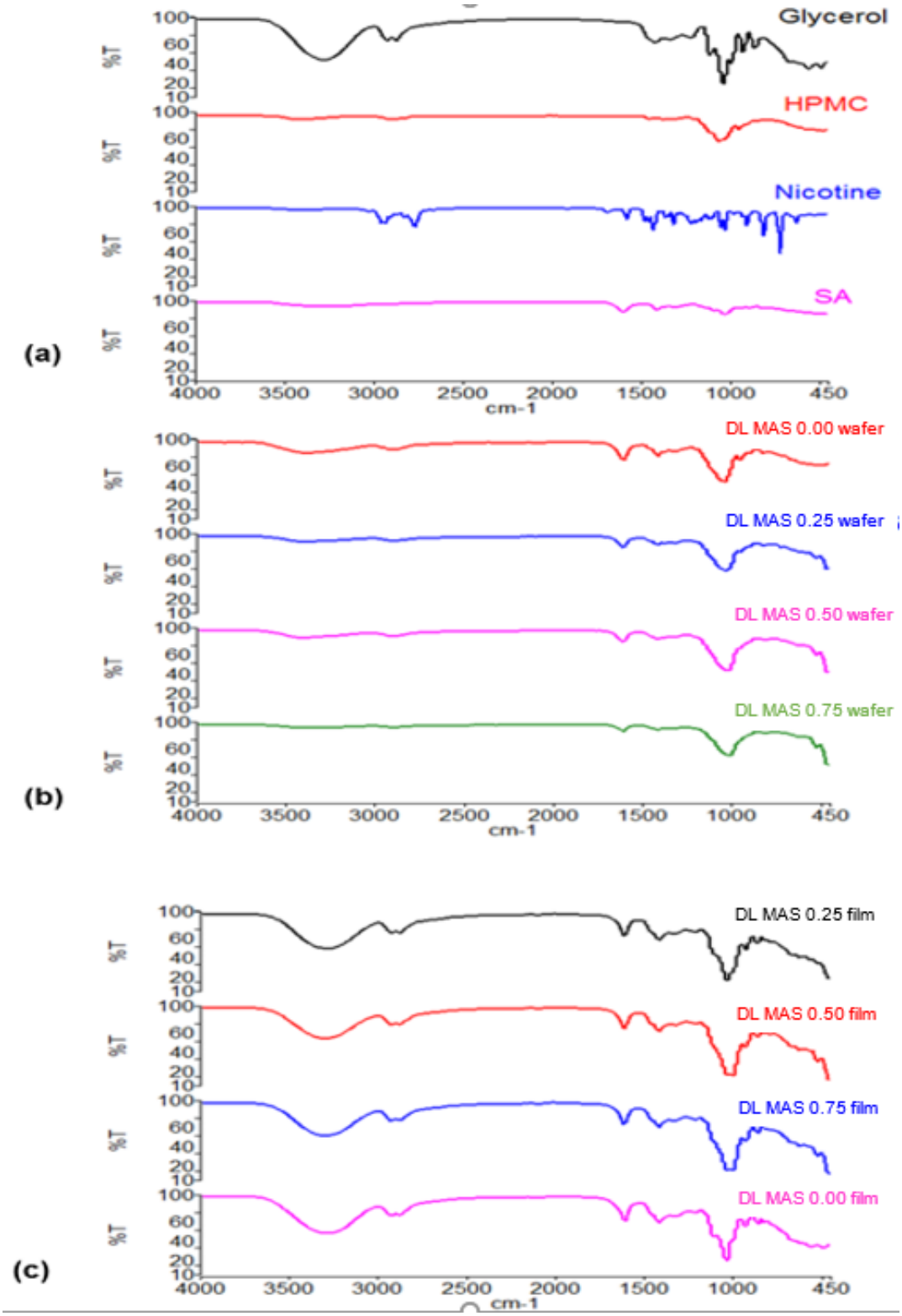

Figure 4 ATR-FTIR spectra of (a) pure polymers, GLY, MAS, and NIC, (b) Drug loaded (DL) MAS wafers and (c) Drug loaded (DL) MAS films.

The characteristic peaks and band assignments of pure polymers, GLY, MAS, NIC, and

NIC loaded composite wafers and films are summarised in Tables A1 and A2 respectively (supplementary data). NIC loaded wafers and films demonstrated a shift to higher wavenumber for O-H, O-C=O (asymmetric) and (symmetric) stretching bands. The Si-O-Al (octahedral Al), characteristic peak of MAS at 517cm^{-1} was demonstrated in MAS loaded wafers, with a shift to higher wavelength at 518cm^{-1}, but showed a shift to lower wavenumber at 516cm^{-1} for the corresponding films. However, films without MAS demonstrated a characteristic C-H peak of GLY with a shift to lower wavenumber and C-CH_3 characteristic peak of HPMC (1314cm^{-1}) with a shift to higher wavenumber (1319cm^{-1}).

3.7 Swelling

Figure 5 shows the swelling profiles of both composite wafers and films containing different concentrations of MAS. Wafers demonstrated a rapid and higher swelling profile (Figure 5a) compared to films (Figure 5b). A swelling index between 700 - 1150% was observed in wafers and 150 - 700% in films after 2 mins of contact with PBS solution. Increase in swelling index with incorporation of MAS was demonstrated in both wafers and films. Although MAS wafers (i.e. MAS 0.25, 0.50 and 0.75) showed higher swelling index than wafers with no MAS (i.e. MAS 0.00), wafers with MAS 0.75 concentration showed the lowest swelling index among but was still significantly higher ($p=0.0035$) than the wafers with no MAS present. In the same way, films with MAS 0.75 also showed the lowest swelling among the composite films but was still significantly higher ($p=0.0118$) than the films without MAS.

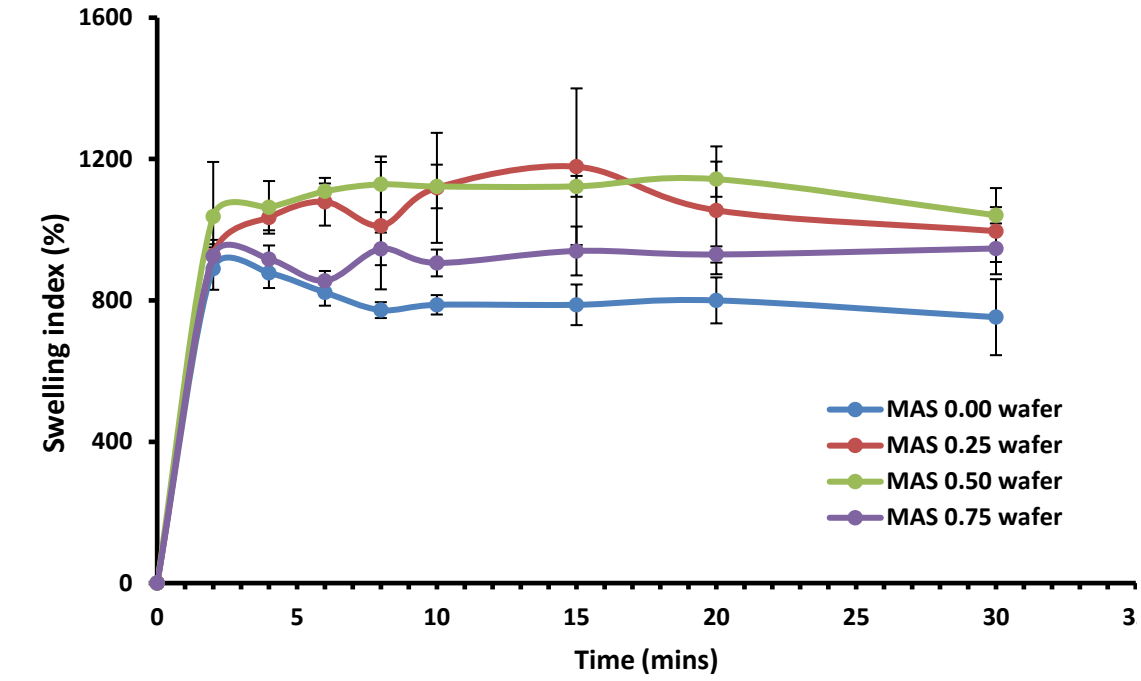

(a)

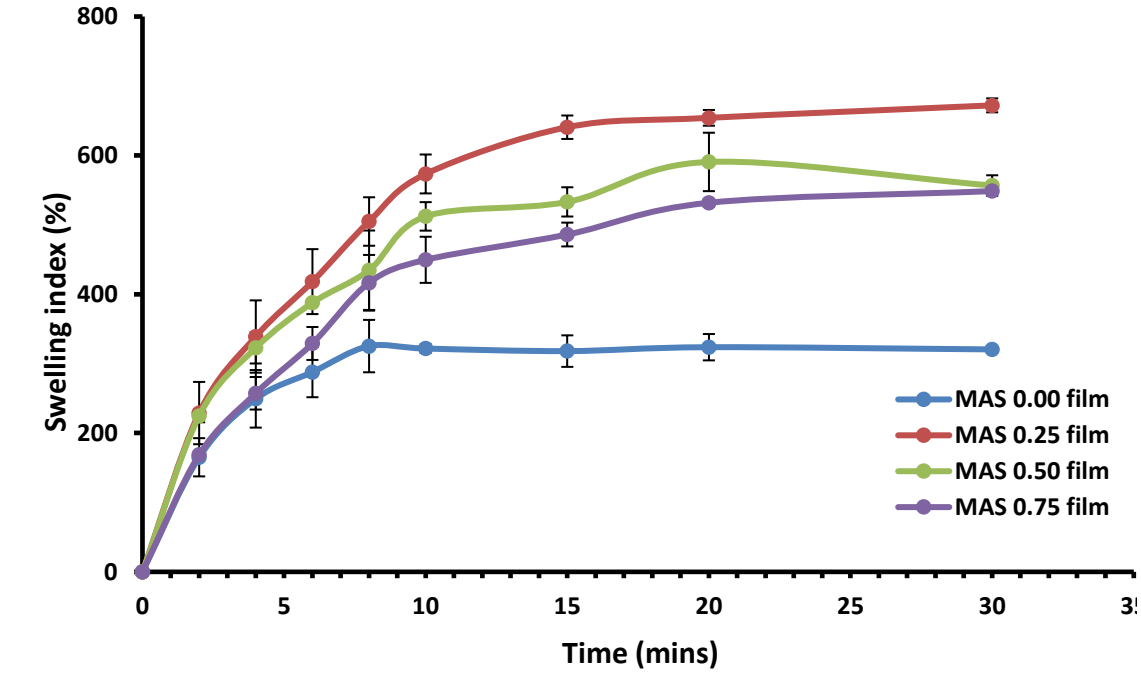

(b)

386 **Figure 5** Swelling profiles (i.e. swelling index (%) against time) (n = 3) of (a) wafers and (b)
387 films.

3.8 Mucoadhesion studies

Figure S3 shows the adhesive properties [(PAF, TWA and cohesiveness (stickiness)] of NIC loaded wafers and films. The wafers showed a significant ($p < 0.05$) decrease in PAF from 1.29 ± 0.22N for MAS 0.00 wafer to 0.23 ± 0.003N for MAS 0.25 wafer, representing about 82% decrease in adhesive force but remained constant with further increase in MAS concentration. NIC loaded films on the other hand, demonstrated an increase in PAF as MAS increased. Films showed an increase from 1.94±0.13N for MAS 0.00 formulation to 2.44 ± 0.44N for MAS 0.75. In general, there was a significant difference ($p < 0.05$) in PAF between NIC loaded wafer and film, with the films showing higher PAF compared to their corresponding wafers (Figure S3a). The TWA (Figure S3b) of NIC loaded wafers also demonstrated an initial decrease from 1.01 ± 0.21Nmm for MAS 0.00 to 0.17 ± 0.025Nmm for MAS 0.25, and then remained constant as MAS concentration increased which was quite similar to the pattern observed for PAF. NIC loaded films however showed an increase in TWA with in the presence of MAS, increasing from 1.74 ± 0.52Nmm for MAS 0.25 to 2.28 ± 0.79 for MAS 0.75. The cohesiveness (stickiness') profiles of NIC loaded wafers and films are shown in Figure S3c. The cohesiveness of wafers increased with the introduction of MAS, with a value of 1.92 ± 0.51mm for MAS 0.00 and 9.96 ± 0.71mm for MAS 0.25. MAS can therefore significantly influence cohesiveness of NIC loaded wafers. However, in NIC film there was no influence, as cohesiveness remained relatively constant as MAS concentration increased.

Overall, although NIC loaded composite wafers demonstrated high cohesiveness (stickiness), NIC loaded MAS films demonstrated better mucoadhesive properties considering the PAF and TWA profiles.

3.9 Drug content (% loading / recovery)

Figure S4 shows the drug content of the composite wafers and films and calculated as percentage drug remaining in the dosage forms after the formulation process. NIC content was 79 ± 1% and 28 ± 4% respectively for wafers and films containing no MAS, which increased to 93% and 92% respectively for wafers and films loaded with MAS 0.25, after which both showed a decrease in NIC content as MAS increased further. The increase in MAS from MAS 0.00 to 0.25 had the most significant effect on the NIC content of SA based composite films, with an increase of approximately 70% compared to wafers which increased by 15%. Further, the subsequent decrease in NIC content in composite films as MAS concentration increased, was more pronounced than the corresponding wafers. In the case of wafers, three formulations MAS 0.25 wafers, MAS 0.50 wafers and MAS 0.75 wafers maintained the NIC content above 85% whilst only MAS 0.25 films had values above 80%. Due to the very low drug content for MAS films at MAS 0.00, these films were not employed during *in vitro* drug dissolution studies.

3.10 In vitro drug dissolution

Figure 6 shows the drug dissolution profiles of MAS wafers and films. The wafers demonstrated a rapid drug release with about 80-100% of NIC released within 60 mins while films showed a much more sustained release profile with drug gradually released from the polymeric matrix. The different wafer formulations showed similar drug release profiles with no significant difference ($p > 0.05$) observed as MAS concentration increased. However, films demonstrated a significant difference ($p < 0.05$) in percentage cumulative drug release as MAS increased. Films containing MAS 0.25 showed the slowest release rate with a maximum cumulative drug release of 15.1 ± 6.3% at 120 mins followed by MAS 0.50 film (26.1 ± 0.1%) and increased slightly at

437 MAS 0.75 film with a cumulative drug release of 35.6 ± 2.7%.

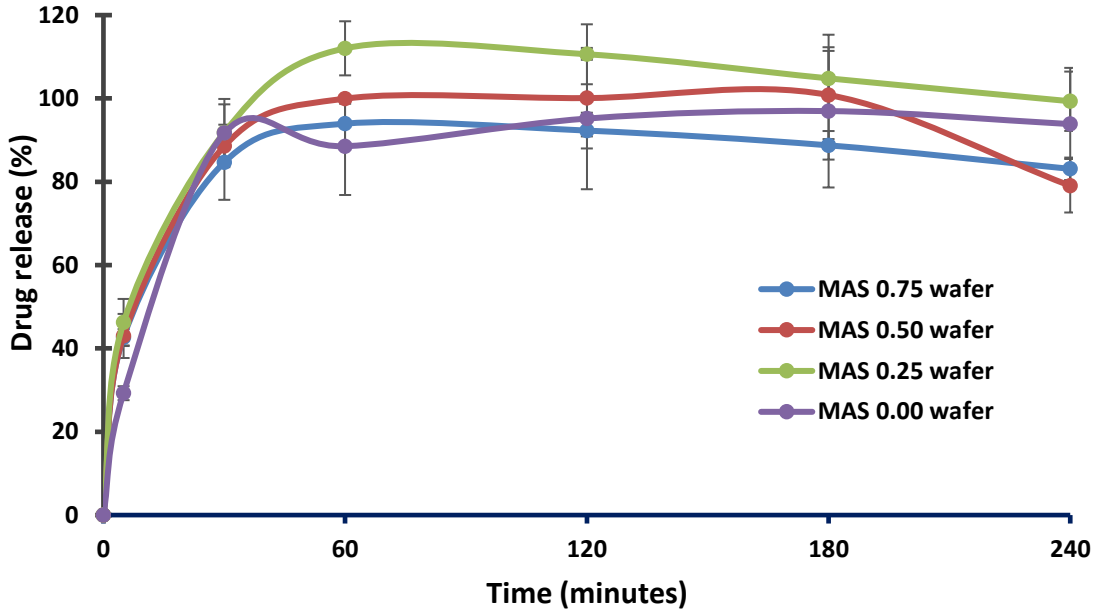

438

439 **(a)**

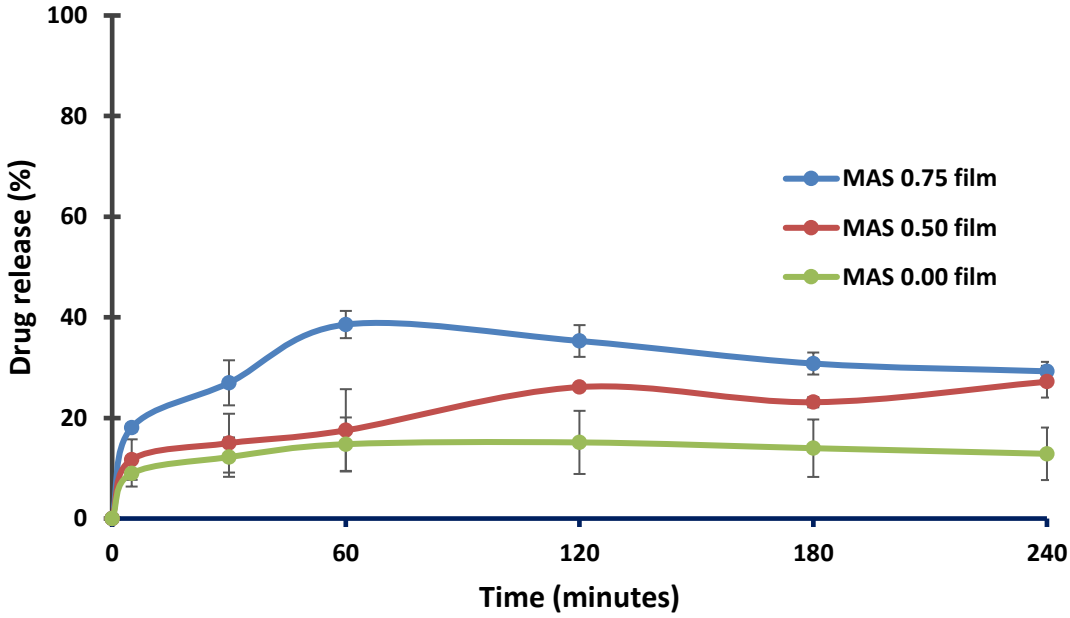

440

441 **(b)**

442 **Figure 6** *In vitro* drug release profiles (n = 3) of NIC loaded (a) wafers and (b) films. containing
443 different MAS concentrations.

3.11 Drug release kinetics

The release parameters of NIC loaded SA based wafers and films have been summarised in Tables A3 and A4 respectively (supplementary data). Based on the R^2 values, drug release from wafers fit the Korsmeyer-Peppas best compared to other models. However, the release data for films fit the Korsmeyer-Peppas equation for MAS 0.75 films (R^2 = 0.8986) and MAS 0.25 films (R^2 = 0.9707) whilst Hixson-Cromwell equation fit the release data for MAS 0.50 films (R^2 = 0.9947). The n values of Korsmeyer-Peppas equation in wafers ranged from 0.3306 - 0.4839 and decreased with increase in MAS in wafers and less than 0.45 except for MAS 0.00 wafers (0.4839). Similar to wafers, films demonstrated an n value of less than 0.45, which ranged from 0.1744 - 0.2363.

4 Discussion

The introduction of MAS into wafers and film and the presence of SA was to overcome the challenges posed by NIC as regards to volatility and poor stability. The increase in surface stickiness, stringiness and gel strength with increase in MAS concentration was the result of decrease in free volume between the HPMC and SA polymers as the concentration of MAS increased.

The mechanical hardness of wafers is related to their handling and friability and therefore consistency of wafer structure can be demonstrated using hardness data as this shows their resistance to compression deformation forces (Boateng & Areago, 2014). The consistency in the hardness for wafers containing MAS 0.00 to 0.50 was attributed to their constant porosities. The decrease in hardness of wafers at higher MAS concentration (MAS 0.75) is due to the increased porosity and low free volume between the polymers due to higher MAS solid particles leading to weaker sponge walls. The

internal microstructure (SEM) also demonstrated weak sponge walls in wafers containing the highest MAS concentration (MAS 0.75). It's been reported that an increase in porosity can reduce hardness as a result of reduced interaction between polymer chains within the network (Boateng et al., 2010).

The tensile properties of films are very important as they affect ease of handling and application. Pongjanyakul and co-workers demonstrated the effect of MAS on elongation and tensile strength, concluding that addition of solid particles usually decreases films' elongation (Pongjanyakul et al 2005). SA based films showed a decrease in percentage elongation with MAS because MAS reduces the free volume between SA and HPMC (Table 1) which further resulted in the increase in brittleness (tensile strength) and stiffness (elastic modulus). This could imply that MAS had an opposite effect to the known plasticising action of GLY.

The physical form of formulations (amorphous or crystalline) can influence functional characteristics such as water uptake and mucoadhesion (Prabaharan & Gong, 2008). The crystalline peaks demonstrated in both wafers and films were due to the crystalline nature of the montmorillonite and saponite clay structures of MAS. Although, crystallinity generally decreases dissolution rate, incorporation of MAS increased the swelling index due to the interaction between MAS and SA as demonstrated in ATR-FTIR results and also previously reported (Pongjanyakul et al., 2005). MAS can interact with SA through the formation of hydrogen bonding between surface silanol groups of MAS and the carboxyl groups of SA and the extent of this interaction is responsible for the observed changes in characteristics with increase in MAS concentration.

Suitable hydration and swelling play a major role in mucoadhesion as well as drug release patterns (Pawar, Tetteh, & Boateng, 2013). In general, the rapid swelling

494 profile of wafers compared to films was the result of the sponge-like pores in wafers
495 microstructure, enabling faster water ingress and making them hydrate faster than the
496 films. (Pongjanyakul et al., 2005) suggested that the decrease in water uptake in SA
497 films loaded with MAS was due to the interaction of SA and MAS, which produced a
498 denser matrix structure and this could have occurred in the case of the films formulated
499 in this study.

500 SA based films showed higher mucoadhesion than the corresponding wafers due
501 to the presence of GLY. This allowed better contact stage via hydrogen bonding and
502 van der Waals forces (adsorption theory of mucoadhesion) than wafers which were
503 based on the diffusion theory (Smart, 2005). The increase in mucoadhesion in films as
504 MAS concentration increased could be attributed to the exposure of weak positive and
505 negatively charged forces. Upon contact with physiological fluids, the charged MAS
506 interacts with mucin macromolecules leading to increased van der Waals forces and
507 electrostatic interactions (Pongjanyakul & Suksri, 2009, Rowe et al., 2006). The
508 decrease in mucoadhesion of wafers as MAS concentration increased could be due to
509 the poor contact stage caused by gaps related to the sponge-like pores present in wafers
510 (Smart, 2005). In addition, MAS can compete with SA and NIC for binding mucin.
511 However, the increase in MAS showed no noticeable change in adhesion, as the freely
512 available MAS after interaction with NIC, interacts with SA, therefore reducing the
513 availability of the SA cationic group to interact with mucin.

514 The primary aim of incorporating MAS into HPMC-SA wafers and films was to
515 stabilise NIC. The volatility of NIC base is one of the main reasons for its instability in
516 formulations as NIC evaporates at high temperature during the drying process (Nair et
517 al., 1997). MAS can readily interact with amine based drugs through electrostatic
518 interactions which can improve NIC stability (Pongjanyakul & Suksri, 2009). However,

519 higher percentage NIC content was observed in wafers than in the films due to the lower
520 temperatures used during freeze-drying, compared oven drying. The decrease in
521 percentage NIC content in MAS wafers and films at MAS 0.50 and 0.75 can be
522 explained by the increase in repulsive forces which build-up as MAS concentration
523 increased.

524 The release of drug from polymeric matrices such as wafers and films is
525 dependent on factors such as hydration and eventual swelling of the polymeric dosage
526 form (Siepmann & Peppas, 2012). As formulations come in contact with dissolution
527 medium, they undergo hydration, swelling and erosion (dissolution), which was evident
528 in the swelling behaviour of the various wafers and films. The rapid release (80 - 100%
529 in 60 mins) of the wafers corresponded to the high swelling index, due to the sponge-
530 like porous internal structure of wafers (SEM and percentage porosity). Therefore, the
531 use of SA based wafers can be efficient in achieving rapid release of NIC to the buccal
532 mucosa to ensure rapid easing of the urge to smoke tobacco. The much slower release
533 of NIC from the films, which corresponded to low swelling index, can be important in
534 achieving sustained release of NIC, with an extended effect to reduce the need for
535 frequent administration. The release exponents of MAS loaded formulations of less than
536 0.45 was outside the limits of Korsmeyer-Peppas model and also highlights the
537 limitations of the Korsmeyer-Peppas model in the understanding of drug release
538 mechanisms (Shoaib, Tazeen, Merchant, & Yousuf, 2006). However, the release
539 exponent of 0.48 for wafers without MAS (MAS 0.00 wafers) shows that drug release
540 from these wafers followed a Fickian diffusion transport mechanism (Nair et al., 2013).

541 **5 Conclusions**

542 Composite SA based films and wafers, incorporating MAS have been successfully

formulated as potential buccal delivery systems for NRT. The two formulations demonstrated different behaviours in their functional physical characteristics. The wafers showed a porous internal morphology which contribute to higher swelling index than continuous sheet of films. MAS improved the physical stability of NIC with an increase in drug loading capacity via molecular interaction between the inorganic clay and the alkaline drug. The release of drug from the wafers was rapid while release from the corresponding films was sustained. The MAS stabilized formulations have great potential as buccal delivery systems for NRT.

References

Adhikari, S.N.R., Nayak, B.S., Nayak, A.K. & Mohanty, B. (2010). Formulation and evaluation of buccal patches for delivery of atenolol. *AAPS PharmSciTech, 11*, 1038-1044.

Adrian, C.L., Olin, H.B.D., Dalhoff, K. & Jacobsen, J. (2006). In vivo human buccal permeability of nicotine. *International Journal of Pharmaceutics, 311*, 196-202.

Aguzzi, C., Cerezo, P., Viseras, C. & Caramella, C. (2007). Use of clays as drug delivery systems: Possibilities and limitations. *Applied Clay Science, 36*, 22-36.

Benowitz, N.L., Jacob, P. & Savanapridi, C. (1987). Determinants of nicotine intake while chewing nicotine polacrilex gum. *Clinical Pharmacology & Therapeutics, 41*, 467-473.

Boateng, J.S. & Areago, D. (2014). Composite Sodium Alginate and Chitosan Based Wafers for Buccal Delivery of Macromolecules. *Austin Journal of Analytical and Pharmaceutical Chemistry, 1*, 1022.

Boateng, J.S., Auffret, A.D., Matthews, K.H., Humphrey, M.J., Stevens, H.N.E. & Eccleston, G.M. (2010). Characterisation of freeze-dried wafers and solvent evaporated films as potential drug delivery systems to mucosal surfaces. *International Journal of Pharmaceutics, 389*, 24-31.

Boateng, J.S. & Okeke, O. (2014). Chitosan-based films for the sustained release of peptides: a new era in buccal delivery? *Therapeutic delivery, 5*, 497-500.

Dash, S., Murthy, P.N., Nath, L. & Chowdhury, P. (2010). Kinetic modeling on drug release from controlled drug delivery systems. *Acta Pol Pharm, 67*, 217-223.

Gilman, J.W. (1999). Flammability and thermal stability studies of polymer layered-silicate (clay) nanocomposites1. *Applied Clay Science, 15*, 31-49.

Khan, S., Boateng, J.S., Mitchell, J. & Trivedi, V. (2015). Formulation, Characterisation and Stabilisation of Buccal Films for Paediatric Drug Delivery of Omeprazole. *AAPS PharmSciTech*, 1-11.

Manivannan, R., Balasubramaniam, A., Anand, D.C., Sandeep, G. & Rajkumar, N. (2008). Formulation and in-vitro evaluation of mucoadhesive buccal tablets of diltiazem hydrochloride. *Research Journal of Pharmacy and Technology, 1*, 478-480.

Mihranyan, A., Andersson, S.-B. & Ek, R. (2004). Sorption of nicotine to cellulose powders. *European Journal of Pharmaceutical Sciences, 22*, 279-286.

Morales, J.O. & McConville, J.T. (2011). Manufacture and characterization of mucoadhesive buccal films. *European Journal of Pharmaceutics and Biopharmaceutics, 77,* 187-199.

Nair, A.B., Kumria, R., Harsha, S., Attimarad, M., Al-Dhubiab, B.E. & Alhaider, I.A. (2013). In vitro techniques to evaluate buccal films. *Journal of Controlled Release, 166*, 10-21.

Nair, M.K., Chetty, D.J., Ho, H. & Chien, Y.W. (1997). Biomembrane permeation of nicotine: Mechanistic studies with porcine mucosae and skin. *Journal of Pharmaceutical Sciences, 86,* 257-262.

Okeke O.C., Boateng, J.S. (2016). Composite HPMC and sodium alginate based buccal formulations for nicotine replacement therapy. *International Journal of Biological Macromolecules*. *91*, 31-44.

Pandey, S.L., Hingawe, N.T., Das, U. & Patil, A.T. (2014). Mucoadhesive buccal tablets of domperidone: formulation evaluation and effects of process variables. *Journal of Pharmaceutical Investigation, 44,* 103-110.

Pavlidou, S. & Papaspyrides, C.D. (2008). A review on polymer-layered silicate nanocomposites. *Progress in Polymer Science (Oxford), 33*, 1119-1198.

Pawar, H.V., Tetteh, J. & Boateng, J.S. (2013). Preparation, optimisation and characterisation of novel wound healing film dressings loaded with streptomycin and diclofenac. *Colloids and Surfaces B: Biointerfaces, 102*, 102-110.

Pongjanyakul, T., Priprem, A. & Puttipipatkhachorn, S. (2005). Investigation of novel alginate− magnesium aluminum silicate microcomposite films for modified-release tablets. *Journal of Controlled Release, 107,* 343-356.

Pongjanyakul, T. & Suksri, H. (2009). Alginate-magnesium aluminum silicate films for buccal delivery of nicotine. *Colloids and Surfaces B: Biointerfaces, 74*, 103-113.

Pongjanyakul, T. & Suksri, H. (2010). Nicotine-loaded sodium alginate–magnesium aluminum silicate (SA–MAS) films: Importance of SA–MAS ratio. *Carbohydrate Polymers*, 80, 1018-1027.

Prabaharan, M. & Gong, S. (2008). Novel thiolated carboxymethyl chitosan-g-β-cyclodextrin as mucoadhesive hydrophobic drug delivery carriers. *Carbohydrate Polymers, 73,* 117-125.

Rakić, V., Damjanović, L., Rac, V., Stošić, D., Dondur, V. & Auroux, A. (2010). The adsorption of nicotine from aqueous solutions on different zeolite structures. *Water Research, 44,* 2047-2057.

Rowe, R.C., Sheskey, P.J., Owen, S.C. & American Pharmacists, A. (2006). *Handbook of Pharmaceutical Excipients.* Pharmaceutical Press.

Sattar, M., Sayed, O.M. & Lane, M.E. (2014). Oral transmucosal drug delivery – Current status and future prospects. *International Journal of Pharmaceutics, 471,* 498-506.

Shoaib, M.H., Tazeen, J., Merchant, H.A. & Yousuf, R.I. (2006). Evaluation of drug release kinetics from ibuprofen matrix tablets using HPMC. *Pakistan Journal of Pharmaceutical Sciences, 19,* 119-124.

Siepmann, J. & Peppas, N.A. (2012). Modeling of drug release from delivery systems based on hydroxypropyl methylcellulose (HPMC). *Advanced Drug Delivery Reviews, 64,* Supplement, 163-174.

Singhvi, G. & Singh, M. (2011). Review: in-vitro drug release characterization models. *International Journal of Pharmacy Studies Research, 2,* 77-84.

Smart, J.D. (2005). The basics and underlying mechanisms of mucoadhesion. *Advanced Drug Delivery Reviews, 57,* 1556-1568.

İkinci, G., Şenel, S., Wilson, C.G. & Şumnu, M. (2004). Development of a buccal bioadhesive nicotine tablet formulation for smoking cessation. *International Journal of Pharmaceutics, 277,* 173-178.